ELSEVIER

International Journal of Minerals, Metallurgy and Materials
Volume 16, Number 5, October 2009, Page 608

Materials

Band gaps of elastic waves in 1-D phononic crystals with imperfect interfaces

Min Zheng and Pei-jun Wei

School of Applied Science, University of Science and Technology Beijing, Beijing 100083, China
(Received 2008-10-16)

Abstract: Band gaps of elastic waves in 1-D phononic crystals with imperfect interfaces were studied. By using the transfer matrix method (TMM) and the Bloch wave theory in the periodic structure, the dispersion equation was derived for the periodically laminated binary system with imperfect interfaces (the traction vector jumps or the displacement vector jumps). The dispersion equation was solved numerically and wave band gaps were obtained in the Brillouin zone. Band gaps in the case of imperfect interfaces were compared with that in the case of perfect interfaces. The influence of imperfect interfaces on wave band gaps and some interesting phenomena were discussed.

Key words: phononic crystal; transfer matrix; band gap; imperfect interface; Bloch wave

[*This work was financially supported by the National Natural Science Foundation of China (No.10672019).*]

1. Introduction

Phononic crystals, also called acoustic band gap materials, are composite elastic media constituted of periodic repetitions of different solids. The acoustic band gap is one of important properties of phononic crystals. When composite incident waves with various frequencies run into the phononic crystal, the waves with frequency falling into the pass band can propagate through the phononic crystal but the waves with frequency falling into the forbidden band can not propagate through. The filtering property of phononic crystals is why it is called acoustic band gap materials. The potential application of the band gap property in civil and military engineering makes the phononic crystal receive more and more attention in the past ten years [1-7]. It is noted that most of these studies on phononic crystals focused on two aspects. One is the calculation method of band gaps. The other is the forming mechanism of band gaps. In addition, in order to design the desired acoustic band gap, the effect of the topology structure of composites and the contrast of material constants were also investigated extensively [1-2]. The main methods studying phononic crystals at present include the transfer matrix method [6-7], the plane wave expansion method [3], the finite time domain difference method [4], and the multiple scattering method [5]. For one dimensional phononic crystals, the transfer matrix method was usually used due to the laminated feature. The interface in composite materials plays an important role. The interacting of waves and interfaces can influence the wave propagation in a composite material evidently. When the transfer matrix was derived, the continuous condition of displacement vector and traction vector across the interface was usually used. This means the interface is perfect, namely, the joint is fast, which ensures both displacement and traction are continuous across the interface [8-11]. However, the joint between two different solids is often not so fast due to various damages and defects in actual situation [12]. The influence of imperfect interfaces on band gaps is not investigated up to now. In this paper, imperfect interfaces, namely, the displacement or the traction vector jumps across the interfaces, are considered. The influence of imperfect interfaces on wave bands and band gaps is discussed based on the comparison of numerical results obtained from perfect interfaces and imperfect interfaces. The feature of phononic crystals with imperfect interfaces is also investigated.

2. Transfer matrix in the case of perfect

Corresponding author: Pei-jun Wei , **E-mail:** weipj@sas.ustb.edu.cn
Also available online at www.sciencedirect.com

interfaces

Consider a one-dimensional phononic crystal of laminated structure formed by periodic repetition of two different solids, see Fig. 1. The x axis is perpendicular to the planar interface of two solids and the yoz coordinate plane is parallel to the planar interface. The thicknesses of two solids are a_1 and a_2, respectively. The elastic constants and mass densities of two isotropic solids are denoted by λ_j, μ_j and ρ_j (j=1, 2), respectively.

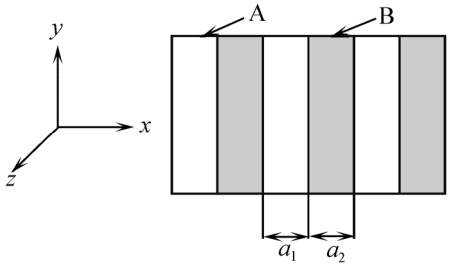

Fig. 1. One dimensional phononic crystal of periodic laminated structure.

For a homogenous, isotropic and linear elastic solid, the motion equation is

$$(\lambda+2\mu)\nabla(\nabla\cdot\boldsymbol{u})-\mu\nabla\times\nabla\times\boldsymbol{u}=\rho\ddot{\boldsymbol{u}} \tag{1}$$

The plane wave propagating along the x axis direction, namely, normal incident wave, can be written as

$$\boldsymbol{u}(r,t)=\boldsymbol{u}(r)\mathrm{e}^{\mathrm{i}\omega t}=u(x)\hat{\boldsymbol{e}}\mathrm{e}^{\mathrm{i}\omega t} \tag{2}$$

Inserting Eq. (2) into Eq. (1) leads to

$$\frac{\partial^2 u(x)}{\partial x^2}+k^2u(x)=0 \tag{3}$$

The solution of Eq. (3) is

$$u(x)=A_1\mathrm{e}^{\mathrm{i}kx}+A_2\mathrm{e}^{-\mathrm{i}kx} \tag{4}$$

Therefore, the stress can be obtained by

$$\sigma=\mathrm{i}\rho c^2k\left(A_1\mathrm{e}^{\mathrm{i}kx}-A_2\mathrm{e}^{-\mathrm{i}kx}\right) \tag{5}$$

For incident SH wave,

$u(x)=u_z(x)$, $\hat{\boldsymbol{e}}=\hat{\boldsymbol{e}}_z$, $k=k_\mathrm{t}=\omega/c_\mathrm{t}$, $c_\mathrm{t}=\sqrt{\mu/\rho}$, $\sigma=\sigma_{xz}=\mu\dfrac{\partial u}{\partial x}$.

For incident P wave,

$u(x)=u_x(x)$, $\hat{\boldsymbol{e}}=\hat{\boldsymbol{e}}_x$, $k=k_\mathrm{l}=\omega/c_\mathrm{l}$,

$c_l=\sqrt{(\lambda+2\mu)/\rho}$, $\sigma=\sigma_{xx}=(\lambda+2\mu)\dfrac{\partial u}{\partial x}$.

A perfect interface means the displacement and the traction vectors are continuous along the normal and tangent direction of the planar interface. The boundary condition on the interface can be written as

$$[\boldsymbol{t}]=0,\quad [\boldsymbol{u}]=0 \tag{6}$$

where $[\cdot]$ denotes the jump across interface, $[\boldsymbol{t}]=\boldsymbol{t}^+-\boldsymbol{t}^-$ denotes the traction vector jump, and $[\boldsymbol{u}]=\boldsymbol{u}^+-\boldsymbol{u}^-$ denotes the displacement vector jump. $\boldsymbol{t}^+$, $\boldsymbol{t}^-$, $\boldsymbol{u}^+$ and $\boldsymbol{u}^-$ denote the displacement and traction vectors on both sides of the interface, respectively. The component form of Eq. (6) can be written as

$$\begin{aligned}&\sigma_{xs,1\mathrm{R}}^{(i)}=\sigma_{xs,2\mathrm{L}}^{(i)},\quad u_{s,1\mathrm{R}}^{(i)}=u_{s,2\mathrm{L}}^{(i)}\\&\sigma_{xs,2\mathrm{R}}^{(i)}=\sigma_{xs,1\mathrm{L}}^{(i+1)},\quad u_{s,2\mathrm{R}}^{(i)}=u_{s,1\mathrm{L}}^{(i+1)}\end{aligned} \tag{7}$$

where $s=x,z$. Subscript 1 and 2 denote two different solids (solid A and solid B). Subscript L and R denote the left and right surfaces of each solid. A composite layer constituted of solid A and solid B is called an element layer and is denoted by i (i=1, 2,···, n). Solid A and solid B is called sub-layer (denoted by j(j=1, 2)) of an element layer. The state vector of the left or right surface of each sub-layer is defined as

$$\begin{cases}\boldsymbol{V}_{j\mathrm{L}}^{(i)}=\left\{u_{z,j\mathrm{L}}^{(i)},\sigma_{zx,j\mathrm{L}}^{(i)}\right\}^{\mathrm{T}}\\ \boldsymbol{V}_{j\mathrm{R}}^{(i)}=\left\{u_{z,j\mathrm{R}}^{(i)},\sigma_{zx,j\mathrm{R}}^{(i)}\right\}^{\mathrm{T}}\end{cases}\text{ (for SH wave),}$$

$$\begin{cases}\boldsymbol{V}_{j\mathrm{L}}^{(i)}=\left\{u_{x,j\mathrm{L}}^{(i)},\sigma_{xx,j\mathrm{L}}^{(i)}\right\}^{\mathrm{T}}\\ \boldsymbol{V}_{j\mathrm{R}}^{(i)}=\left\{u_{x,j\mathrm{R}}^{(i)},\sigma_{xx,j\mathrm{R}}^{(i)}\right\}^{\mathrm{T}}\end{cases}\text{ (for P wave)} \tag{8}$$

State vectors of the left and right surface of the same sub-layer are related by

$$\boldsymbol{V}_{j\mathrm{R}}^{(i)}=\boldsymbol{T}_j'\boldsymbol{V}_{j\mathrm{L}}^{(i)} \tag{9}$$

where $\boldsymbol{T}_j'$ is the transfer matrix of a sub-layer:

$$\boldsymbol{T}_j'=\begin{bmatrix}\cos(k_ja_j) & \sin(k_ja_j)/\omega\rho_jc_j\\ \omega\rho_jc_j\sin(k_ja_j) & \cos(k_ja_j)\end{bmatrix} \tag{10}$$

State vectors of the same surface of adjacent element layers are related by

$$\boldsymbol{V}_j^{(i)}=\boldsymbol{T}_i\boldsymbol{V}_j^{(i-1)} \tag{11}$$

where $\boldsymbol{T}_i$ is the transfer matrix of an element layer. For perfect interface, it can be written as

$$\boldsymbol{T}_i=\boldsymbol{T}_1'\boldsymbol{T}_2' \tag{12}$$

3. Transfer matrix in the case of imperfect interfaces

For the imperfect interface, the displacement and the traction vectors do not satisfy the continuous con-

dition. In this paper, three kinds of imperfect interfaces are considered, namely, the spring interface model, the mass interface model, and the spring-mass interface model.

(1) The spring interface model.

For the spring interface model, the traction vector is continuous but the displacement vector jumps. The boundary condition in the spring interface model can be expressed as

$$[\boldsymbol{t}]=0,\quad [\boldsymbol{u}]=\boldsymbol{F}\cdot\boldsymbol{t} \tag{13}$$

where $\boldsymbol{F}$ is a diagonal matrix, namely, $\boldsymbol{F}=\mathrm{diag}\{F_n,F_t\}$. In the interface model, an interphase with elasticity but without thickness is assumed existing between two solids, see Fig. 2. The spring coefficient is denoted by $F_s\,(s=n,t)$. If $F_s\to 0$, Eq. (13) reduces to Eq. (6), namely, the imperfect interface reduces to a perfect interface. If $F_s\to\infty$, the imperfect interface is correspond to the debonded case. The boundary condition (13) leads to the following relation between the state vectors:

$$\boldsymbol{V}_{2\mathrm{L}}^{(i)},=\boldsymbol{T}_3'\boldsymbol{V}_{1\mathrm{R}}^{(i)},\quad \boldsymbol{V}_{1\mathrm{L}}^{(i+1)}=\boldsymbol{T}_4'\boldsymbol{V}_{2\mathrm{R}}^{(i)} \tag{14}$$

where

$$\boldsymbol{T}_3'=\boldsymbol{T}_4'=\begin{bmatrix}1 & F_s\\ 0 & 1\end{bmatrix}.$$

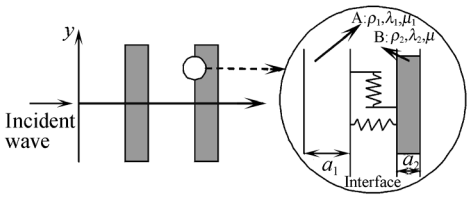

Fig. 2. Spring interface model.

Then, the transfer matrix of an element layer in the case of the spring interface model can be written as

$$\boldsymbol{T}_{\boldsymbol{i}}=\boldsymbol{T}_1'\boldsymbol{T}_3'\boldsymbol{T}_2'\boldsymbol{T}_4' \tag{15}$$

(2) The mass interface model.

For the mass interface model, the displacement vector is continuous but the traction vector jumps. The boundary condition in the case of the mass interface model can be written as

$$[\boldsymbol{u}]=0,\quad [\boldsymbol{t}]=\boldsymbol{M}\cdot\ddot{\boldsymbol{u}}=\boldsymbol{G}\cdot\boldsymbol{u} \tag{16}$$

where $\boldsymbol{M}=\mathrm{diag}\{m_n,m_t\}$, $\boldsymbol{G}=\mathrm{diag}\{-m_n\omega^2,-m_t\omega^2\}$. In the interface model, an interphase with mass but without thickness is assumed existing between two solids, see Fig. 3. When the mass coefficient $G_s=-m_s\omega^2=0\,(s=n,t)$, Eq. (16) reduces to Eq. (6), namely, the imperfect interface reduces to a perfect interface. Similarly, there is relation (14) between state vectors in the case of the mass interface model, but the expression of $\boldsymbol{T}_3'$ and $\boldsymbol{T}_4'$ is replaced by

$$\boldsymbol{T}_3'=\boldsymbol{T}_4'=\begin{bmatrix}1 & 0\\ -G_s & 1\end{bmatrix} \tag{17}$$

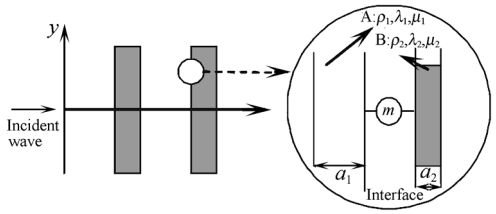

Fig. 3. Mass interface model.

(3) The spring-mass interface model.

For the spring-mass interface model, both displacement and traction vectors jump. The boundary condition in the case of the spring-mass interface model can be written as

$$[\boldsymbol{t}]=\boldsymbol{G}\cdot\langle\boldsymbol{u}\rangle,\quad [\boldsymbol{u}]=\boldsymbol{F}\cdot\langle\boldsymbol{t}\rangle \tag{18}$$

where $\langle\boldsymbol{t}\rangle=(\boldsymbol{t}^{+}+\boldsymbol{t}^{-})/2$, $\langle\boldsymbol{u}\rangle=(\boldsymbol{u}^{+}+\boldsymbol{u}^{-})/2$. In the interface model, an interphase with both elasticity and mass but without thickness are assumed existing between two solids, see Fig. 4. The mass coefficient matrix $\boldsymbol{G}$ and the spring coefficient matrix $\boldsymbol{F}$ are both diagonal matrixes. If $\boldsymbol{G}=0,\boldsymbol{F}=0$, then Eq.(18) reduces to Eq.(6), namely, the imperfect interface reduces to a perfect interface. If $\boldsymbol{G}=0,\boldsymbol{F}\neq 0$, then the imperfect interface reduces to the spring interface model. If $\boldsymbol{F}=0,\boldsymbol{G}\neq 0$, then, the imperfect interface reduces to the mass interface model. Similarly, there is relation (14) between state vectors in the case of the spring-mass interface model, but the expression of $\boldsymbol{T}_3'$ and $\boldsymbol{T}_4'$ is replaced by

$$\boldsymbol{T}_3'=\boldsymbol{T}_4'=\begin{bmatrix}\dfrac{4+F_sG_s}{4-F_sG_s} & \dfrac{4F_s}{4+F_sG_s}\\ \dfrac{4G_s}{4-F_sG_s} & \dfrac{4+F_sG_s}{4-F_sG_s}\end{bmatrix} \tag{19}$$

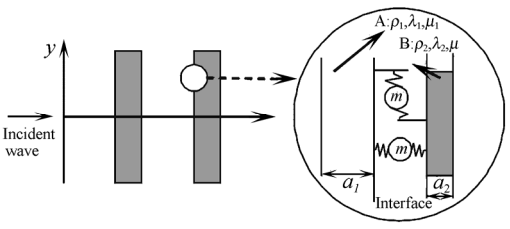

Fig. 4. Spring-mass interface model.

4. Dispersion equation in the case of imper-

fect interfaces

According to the Bloch-Floquet theory in a periodic structure, state vectors on the same sub-layer in adjacent element layers satisfy

$$\boldsymbol{V}_j^{(i)} = \mathrm{e}^{\mathrm{i}ka}\boldsymbol{V}_j^{(i-1)} \tag{20}$$

where $a = a_1 + a_2$ and k is the Bloch wave vector.

Inserting Eq. (11) into Eq. (20) leads to

$$\left|\boldsymbol{T} - \mathrm{e}^{\mathrm{i}ka}\boldsymbol{I}\right| = 0 \tag{21}$$

The dispersion equation in the case of perfect interface can be obtained by inserting $\boldsymbol{T} = \boldsymbol{T}_i = \boldsymbol{T}_1'\boldsymbol{T}_2'$ into Eq. (21). The dispersion equation in the case of imperfect interfaces can be obtained by inserting $\boldsymbol{T} = \boldsymbol{T}_i = \boldsymbol{T}_1'\boldsymbol{T}_3'\boldsymbol{T}_2'\boldsymbol{T}_4'$ into Eq. (21) instead.

(1) The dispersion equation in the case of perfect interfaces.

$$\cos(ka) = \cos(k_1a_1)\cos(k_2a_2) - \frac{1}{2}\left(W + \frac{1}{W}\right)\sin(k_1a_1)\sin(k_2a_2) \tag{22}$$

where $k_j = \omega/c_j\ (j = 1,2)$ is the wave number in two sub-layers, $W = \rho_1c_1/\rho_2c_2$ is the resistance ratio of the two sub-layers.

(2) The dispersion equation in the case of imperfect interfaces.

The spring interface model:

$$\cos(ka) = \cos(k_1a_1)\cos(k_2a_2) - \frac{1}{2}\left(W + \frac{1}{W}\right)\sin(k_1a_1)\sin(k_2a_2) + F_s\left[\mathrm{i}w_1\sin(k_1a_1)\cos(k_2a_2) + \mathrm{i}w_2\cos(k_1a_1)\sin(k_2a_2)\right] - \frac{1}{2}F_s^2w_1w_2\sin(k_1a_1)\sin(k_2a_2) \tag{23}$$

where F_s is the flexibility coefficient of the spring, $w_1 = \mathrm{i}\omega\rho_1c_1, w_2 = \mathrm{i}\omega\rho_2c_2$.

The mass interface model:

$$\cos(ka) = \cos(k_1a_1)\cos(k_2a_2) - \frac{1}{2}\left(W + \frac{1}{W}\right)\sin(k_1a_1)\sin(k_2a_2) + \mathrm{i}G_s\left[\frac{1}{w_1}\sin(k_1a_1)\cos(k_2a_2) + \frac{1}{w_2}\cos(k_1a_1)\sin(k_2a_2)\right] - \frac{G_s^2}{2w_1w_2}\sin(k_1a_1)\sin(k_2a_2) \tag{24}$$

where G_s is the mass coefficient.

The spring-mass interface model:

$$\cos(ka) = \frac{1}{(4 - F_sG_s)^2}\left\{\left[(4 + F_sG_s)^2 + 16F_sG_s\right]\cos(k_1a_1)\cos(k_2a_2) - \frac{1}{2}\left[(4 + F_sG_s)^2\left(W + \frac{1}{W}\right) + 16\left(F_s^2w_1w_2 + \frac{G_s^2}{w_1w_2}\right)\right]\sin(k_1a_1)\sin(k_2a_2) + 4(4 + F_sG_s)i\left[\left(F_sw_1 + \frac{G_s}{w_1}\right)\sin(k_1a_1)\cos(k_2a_2) + \left(F_sw_2 + \frac{G_s}{w_2}\right)\cos(k_1a_1)\sin(k_2a_2)\right]\right\} \tag{25}$$

5. Numerical results and discussion

Consider a phononic crystal composed of Pb and epoxy. The thickness ratio of the Pb sub-layer and the epoxy sub-layer is 1, namely, the filling fraction $f = a_{\mathrm{Pb}}/a = 0.5$, where a_{Pb} is the thickness of the Pb sub-layer, a (=20 mm) is the lattice constant. The material constants of Pb and epoxy are given in Table 1. In the case of imperfect interfaces, numerical results are obtained for the given spring coefficient and the mass coefficient which are listed in Table 2.

Table 1. Material parameters of Pb and epoxy

Material	Mass density / (kg·m^{-3})	Elastic constants / GPa
Pb	ρ_{Pb}=11600	λ_{Pb}=42.3, μ_{Pb}=14.9
Epoxy	ρ_{epoxy}=1180	λ_{epoxy}=4.43, μ_{epoxy}=1.59

In the case of perfect interfaces, band gaps of one-dimensional phononic crystal considered are shown in Fig. 5. The solid line and the dashed line denote the dispersion curves of SH and P waves, respectively. Shadowed zones denote band gaps or stop bands. In order to show the influence of spring coefficient and mass coefficient in the imperfect interface model, four cases are considered in each imperfect interface model. The spring coefficient and mass coefficient in four cases are listed in Table 2. Wave bands and band gaps of one dimensional phononic crystal with imperfect interface are shown in Fig. 6 (the spring interface model), Fig. 7 (the mass interface model), and Fig. 8 (the spring-mass interface model).

It is noted that two band gaps are observed in the considered frequency range in the perfect interface case. But there is a new band gap appearing between the primary first and second band gaps in the imperfect interface case. This means that there are more band gaps in the case of imperfect interfaces compared with the perfect interface case. It is also noted that the primary first and second band gaps become narrow and the central frequency shifts toward low frequency with the increase in the imperfect degree of the interface, for example, the central frequency and width of the first band gap are 0.6180 and 0.3661, respectively, in Fig. 5 and 0.5733 and 0.3003, respectively, in Fig. 6(c).

Table 2. Spring coefficients and mass coefficients in the case of imperfect interface

F_s (SH wave)	F_s (P wave)	F_s/F_0	m_s	m_s/m_0
$F_{t1}=2.5\times10^{-8}$	$F_{n1}=1.47\times10^{-9}$	0.2	$m_1=1.278\times10^{3}$	0.2
$F_{t2}=1.25\times10^{-7}$	$F_{n2}=7.35\times10^{-9}$	1	$m_2=6.39\times10^{3}$	1
$F_{t3}=2.5\times10^{-7}$	$F_{n3}=1.47\times10^{-8}$	2	$m_3=1.278\times10^{4}$	2
$F_{t4}=1.25\times10^{-6}$	$F_{n4}=7.35\times10^{-8}$	10	$m_4=31.95\times10^{3}$	5

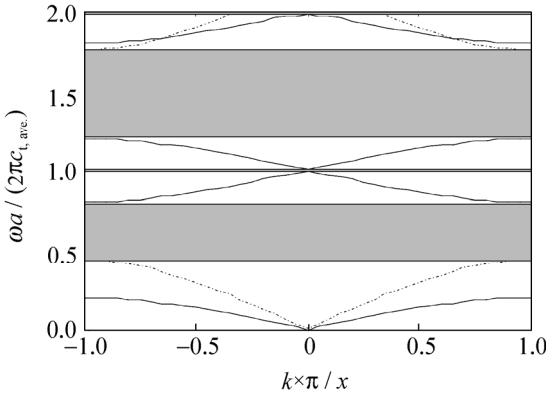

Fig. 5. Band gaps in the case of perfect interfaces (solid lines denote transverse modes and dashed lines denote longitudinal modes, the shadowed regions denote band gaps).

The second band gap has a similar change with the first band gap. However, the new band gap appearing between primary first and second band gaps becomes wide gradually with the increase of the imperfect degree of the interface, although the central frequency shifts toward low frequency still, for example, the central frequency and width of the new band gap are 0.9902 and 0.0289 respectively when $F_s = 0.2F_0$ but 0.9177 and 0.1453 when $F_s = 2F_0$. When the imperfect degree of the interface continues to increase, the total pass band becomes more and more narrow but the total stop band or forbidden band becomes more and more wide.

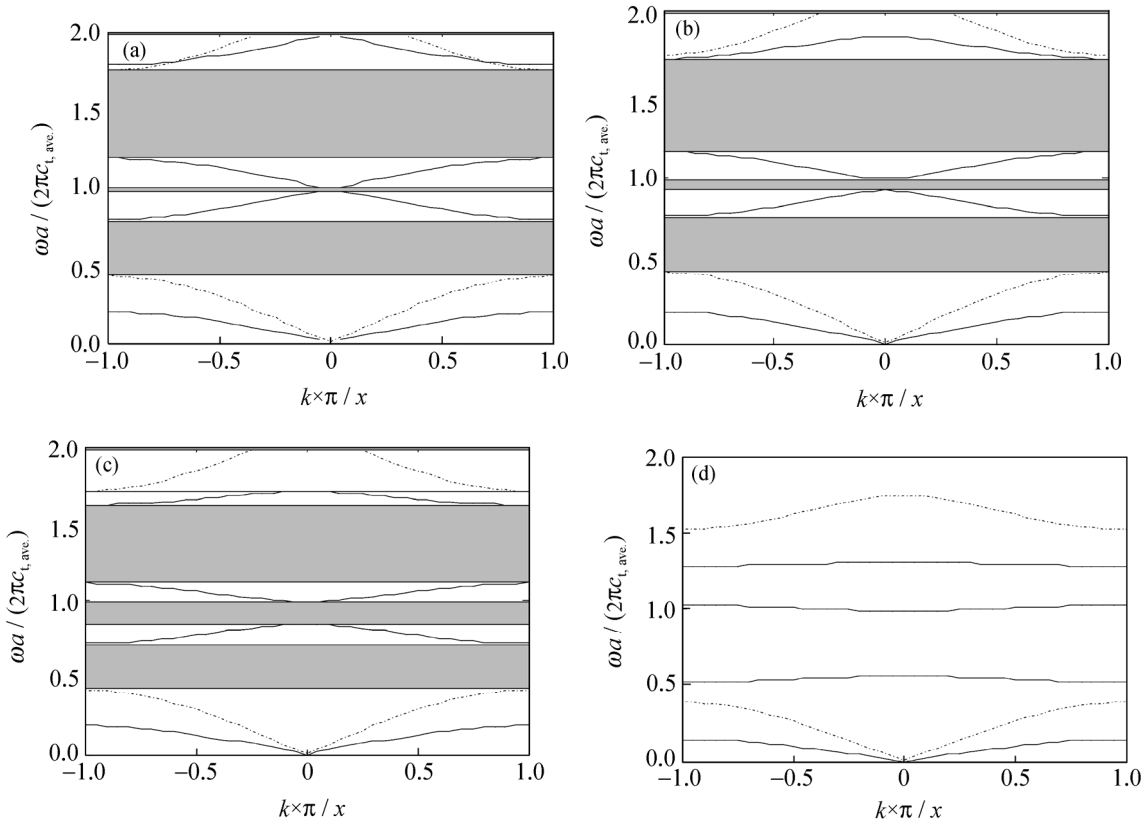

Fig. 6. Band gaps in the case of the spring interface model: (a) F_s=0.2F_0; (b) F_s=F_0; (c) F_s=2F_0; (d) F_s=10F_0.

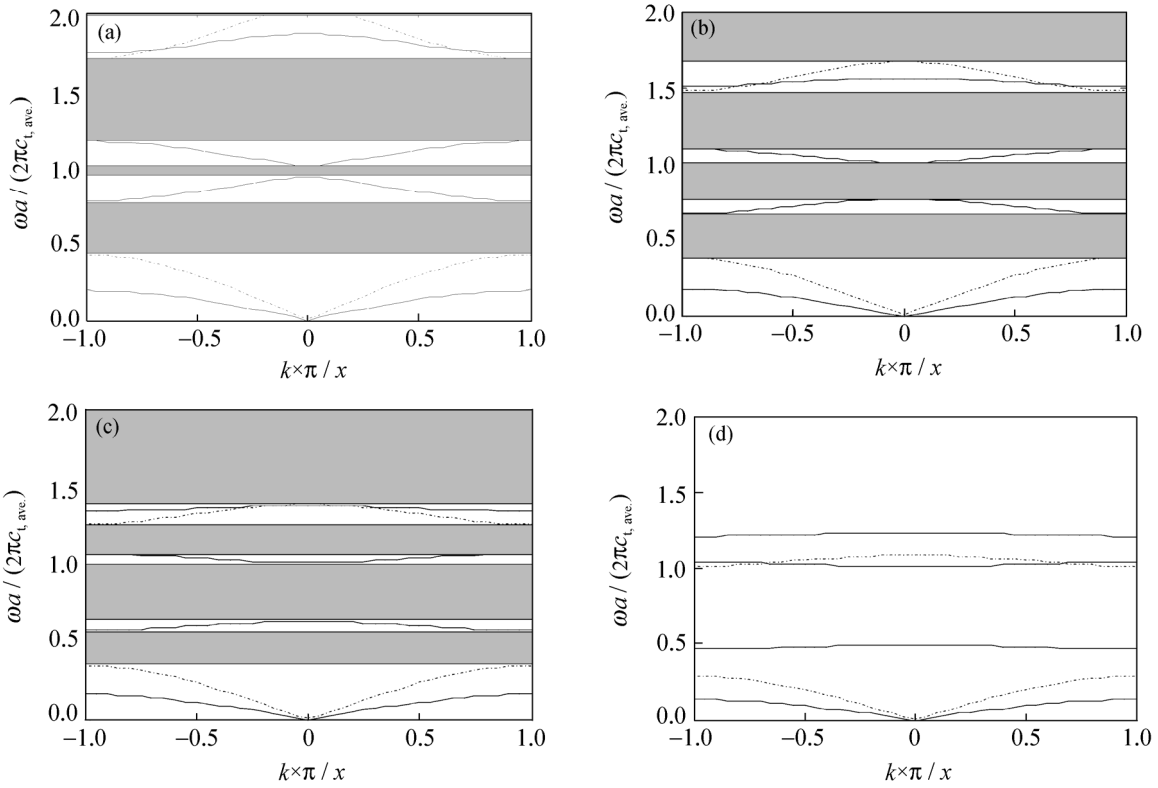

Fig. 7. Band gaps in the case of the mass interface model: (a) G_s=0.2G_0; (b) G_s=G_0; (c) G_s=2G_0; (d) G_s=5G_0.

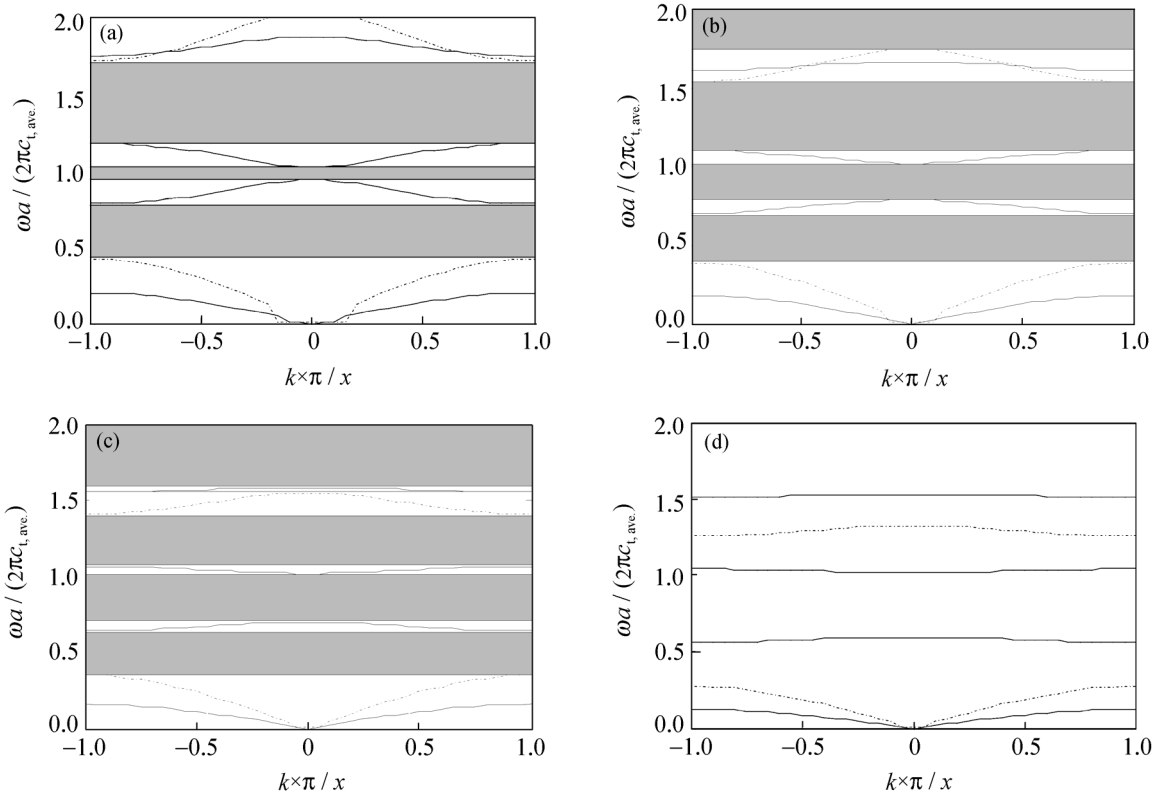

Fig. 8. Band gaps in the case of the spring-mass interface model: (a) F_s=0.2F_0, G_s=0.2G_0; (b) F_s=F_0, G_s=G_0; (c) F_s=2F_0, G_s=2G_0; (d) F_s=10F_0, G_s=5G_0.

In addition, although the first wave band of SH wave and P wave keeps propagating mode, the second, third, and fourth band of SH wave and the second band of P wave evolve gradually from propagating mode to localized mode. The process of evolvement can be observed by comparing (a), (b), (c), and (d) in Figs. 6, 7, and 8. In these wave band figures, the curve denotes the propagating mode and the flat line denotes the localized mode. These flat lines can be seen more clearly in Figs. 6(d), 7(d), and 8(d). It is also noted

that the longitudinal mode is localized more easily in the mass interface model than in the spring interface model. The localized mode is caused by locally resonance and usually appears in the phononic crystal with locally resonant structure, for example, the ternary system [9]. However, in a one-dimension binary phononic crystal with an imperfect interface, the localized modes are also observed. In order to interpret the phenomenon, the imperfect interface can be assumed a special component layer which has mass and elasticity but has no thickness. Thus, the binary phononic crystal with imperfect interfaces is equivalent to the ternary phononic crystal. And the locally resonant structure is formed and the localized mode can exist.

6. Conclusions

(1) There are new band gaps appearing between primary band gaps constantly. Furthermore, these new band gaps become wide gradually with the increase in the imperfect degree of the interface.

(2) Central frequencies of new and old band gaps shift toward low frequency with the increase in the imperfect degree of the interface.

(3) The total width of stop bands in the low frequency range increases in the imperfect interface case compared with the perfect interface case. In contrast, the width of the total pass band decreases. The feature is of importance for the low frequency application of phononic crystals, for example, the damping vibration and suppressing noise.

(4) The localized modes usually appearing in the ternary system are observed in the binary phononic crystal with an imperfect interface. Furthermore, the longitudinal mode is localized more easily in the mass interface model than in the spring interface model. The phenomenon is interpreted by that the imperfect interface leads to the formation of locally resonant structure. Actually, the wider total stop band in the phononic crystal with an imperfect interface is due to the existence of localized modes.

References

[1] S. Zhang and J.C. Cheng, Acoustic band gaps of two-dimensional three-component composite, *Prog. Nat. Sci*., 13(2003), p.809.

[2] Z.Y. Liu, C.T. Chan, and P. Sheng, Three-component elastic wave band-gap material, *Phys. Rev. B*, 65(2002), No.16, p.16511.

[3] M.S. Kushwaha and P. Halevi, Theory of acoustic band structure of periodic elastic composites, *Phys. Rev. B*, 49(1994), No.4, p.2313.

[4] M.M. Sigalas and N. Garcia, Theoretical study of three dimensional elastic band gaps with the finite-difference time-domain methods, *J. Appl. Phys*., 87(2000), No.6, p.3122.

[5] R. Sainidou, N. Stefanou, I.E. Psarobas, *et al*., A layer-multiple scattering method for phononic crystals and hetero structure, *Comput. Phys. Commun.*, 166(2005), p.197.

[6] M.M. Sigalas and C.M. Soukoulis, Elastic-wave propagation through disordered and/or absorptive layered systems, *Phys. Rev. B*, 51(1995), p.2780.

[7] M.I. Hussein, G.M. Hulbert, and R.A. Scott, Dispersive elastodynamics of 1D banded materials and structures: design, *J. Sound Vib.*, 307(2007), p.865.

[8] R.E. Camley, B. Djafari-Rouhani, L. Dobrzynski, *et al.*, Transverse elastic waves in periodically layered infinite and semi-infinite media, *Phys. Rev. B*, 27(1983), No.12, p.7318.

[9] G. Wang, D.L. Yu, J.H. Wen, *et al*., One-dimensional phononic crystals with locally resonant structures, *Phys. Lett. A*, 327(2004), p.512.

[10] A.L. Chen and Y.S. Wang, Study on band gaps of elastic waves propagating in one-dimensional disordered phononic crystals, *Phys. B*, 392(2007), p.369.

[11] F. Kobayashi, S. Biwa, and N. Ohno, Wave transmission characteristics in periodic media of finite length: multilayers and fiber arrays, *Int. J. Solids Struct.*, 41(2004), p.7361.

[12] Y.S. Wang, G.L.Yu, Z.M. Zhang, *et al*., Review on elastic wave propagation under complex interface conditions, *Adv. Mech.* (in Chinese), 30(2000), p.378.